Domain formation and growth in spinodal decomposition of a binary fluid by molecular dynamics simulations

Amol K. Thakre, W. K. den Otter,* and W. J. Briels

Computational Biophysics, Faculty of Science and Technology, University of Twente, P.O. Box 217, 7500 AE Enschede, The Netherlands

The two initial stages of spinodal decomposition of a symmetric binary Lennard-Jones fluid have been simulated by molecular dynamics simulations, using a hydrodynamics-conserving thermostat. By analyzing the growth of the average domain size $R(t)$ with time, a satisfactory agreement is found with the $R(t) \propto t^{1/3}$ Lifshitz-Slyozov growth law for the early diffusion-driven stage of domain formation in a quenched homogeneous mixture. In the subsequent stage of viscous-dominated growth, the mean domain size appears to follow the linear growth law predicted by Siggia.

I. INTRODUCTION

Phase separation and pattern evolution are well-known phenomena visible in various immiscible multicomponent mixtures, ranging from simple liquid mixtures to complex fluids, such as polymers, colloids, surfactants, emulsions, and biological materials [1]. Free-energy minimalization in combination with hydrodynamic flow, collectively known as model H [2–4], determines the global structure of the emerging pattern and the rate at which it evolves. The bicontinuous morphologies observed in the spinodal decomposition of symmetric binary liquids are commonly believed to be self-similar in time, i.e., the patterns at any two moments in time resemble one another and differ only by a scaling factor. This dynamical scaling hypothesis implies that a single time-dependent characteristic length $R(t)$ can be used to characterize the growth of the pattern. It is generally accepted that this evolution follows a simple power law, $R(t) \sim t^{\alpha}$, where α is the growth exponent. Since the coupled and nonlinear differential equations for the composition and flow fields in model H cannot be solved analytically, a comparison of the dominant terms in these equations has led to the identification of three successive growth regimes,

$$R(t) \propto \begin{cases} t^{1/3} & \text{(diffusive)}, \\ t & \text{(viscous)}, \\ t^{2/3} & \text{(inertial)}. \end{cases} \quad (1)$$

Directly following the spinodal quench of a homogeneous mixture, diffusion is the dominant process driving particles to like particles, culminating in the formation of tiny clusters. The growth law is then given by the Lifshitz-Slyozov mechanism [5], $R(t) \propto (\lambda \gamma t)^{1/3}$, where λ is a diffusive transport coefficient and γ is the interfacial tension of the domain boundaries. Our main objective here will be to study this growth law by molecular dynamics simulations, for reasons outlined below. After the formation of domains with well-defined interfaces, the minimalization of their interfacial energies becomes the driving force behind segregation. Siggia [6] derived that the balance between interfacial and viscous forces

then gives rise to the linear scaling law $R(t) \propto (\gamma t / \eta)$, with η the viscosity of the liquid. During this growth the Reynolds number, $\text{Re} = (\rho / \eta) R (dR/dt)$ with ρ denoting the specific gravity, steadily increases. This led Furukawa [7] and Kendon [8] to predict an inertia-dominated scaling law, $R(t) \propto (\gamma t^2 / \rho)^{1/3}$, as the final stage in the growth process. By comparing the aforementioned scaling laws, a transition from the diffusive to the viscous regime is predicted (denoted by an asterisk) to occur at time $t_{dv}^* \approx (\lambda \eta^3 / \gamma^2)^{1/2}$ and length $R_{dv}^* \approx (\lambda \eta)^{1/2}$, while the viscous regime is succeeded by an inertial regime at time $t_{vi}^* \approx \eta^3 / (\gamma^2 \rho)$ and length $R_{vi}^* \approx (\eta^2 / \rho \gamma)$, corresponding to a Reynolds number $\text{Re}_{vi}^* \approx 1$. These approximate expressions serve as guides in the ongoing experimental and numerical research of spinodal decomposition, to be discussed next, which has largely confirmed the power-law growth of the domains.

In most experimental studies on fluid-fluid phase separation in mixtures of simple liquids [9–11], the spinodal decomposition is initiated by a very shallow quench of a homogeneous system to a temperature barely below the critical temperature. The associated Reynolds numbers are very low, hence the observed scaling follows the viscosity-dominated $\alpha = 1$ scaling law. Since phase separation usually progresses extremely rapidly, the critical slowing down in the vicinity of the critical point is exploited to facilitate the experiments. Liquids with high Schmidt numbers [$\text{Sc} = \eta / (\rho D) = 10^3 - 10^5$, with D the diffusion coefficient] are preferred for the same reason. With these expedients, the rapid diffusion-dominated regime of initial domain formation is just about detectable in mixtures of simple liquids [9,11]. Suspensions of large unlike particles, such as colloids and polymers [12], also display a diffusive $t^{1/3}$ coarsening of the domain size, be it much slower than in fluid-fluid mixtures. The inertia-dominated growth regime has not yet been observed experimentally.

Computer simulations of spinodal decomposition using dedicated Navier-Stokes solvers, such as lattice gas automata and lattice Boltzmann (LB) methods, have confirmed the existence of both linear $\alpha = 1$ [13–15] and sublinear $\alpha = 2/3$ [14,16] growth laws. The transition between both regimes was first studied by Kendon *et al.* [14,17] by performing LB simulations of one fluid mixture over a range of viscosities, thus effectively and efficiently sampling a far wider range of time and length scales than can be accessed by a single simu-

*Corresponding author. w.k.denotter@utwente.nl

lation of a large system. The turnover between both growth regimes occurs surprisingly late, centered around $t_{vi} \sim 10^4 t_{vi}^*$, and is protracted over nearly four orders of magnitude in time. In terms of the Reynolds number, this corresponds to the range $1 \lesssim \mathrm{Re}_{vi} \lesssim 100$. A further discussion of the inertial regime was presented by Love *et al.* [18].

Phase separation of binary fluid mixtures has also been simulated using off-lattice particle-based methods, such as molecular dynamics (MD) [19–21] and dissipative particle dynamics (DPD) [22,23]. In the latter method, proposed a decade ago by Hoogerbrugge and Koelman [24], the hard MD potentials between atoms are replaced by extremely soft interactions between fluid elements, and an ingenious thermostat is introduced to make all forces consistent with Newton's third law, which also lies at the basis of hydrodynamics. The main advantages of these particle-based simulation methods are that they are not based on presuppositions regarding the dynamics or thermodynamics of the system, and that they include the perpetual thermal noise. This way, the mesoscopic properties of the phase separating system emerge naturally from the simulations rather than being imposed via the simulation algorithm. Because of the extremely soft interaction potentials in DPD, a linear growth regime is easily reachable in simulations, especially in the computationally less-demanding two-dimensional systems [22]. Simulations by Jury *et al.* [23], combining one thermodynamic state point with a range of tuned viscosities, even suggest that the first glimpses of the broad transition to the inertial regime are attainable with DPD. The early MD simulations of a binary Lennard-Jones fluid by Ma *et al.* [19] were also reported to have reached the inertial regime. Laradji *et al.* [20] simulated a larger Lennard-Jones system and argued, based on a different analysis of the data, that the growth rate is in the viscous regime instead. Both these simulations employed traditional MD thermostats known to interfere with the consistent buildup of the hydrodynamical flow field, while these hydrodynamic interactions are essential for the viscous growth law. Other simulations with stronger perturbations of the flow field have shown that disturbances may impede viscous domain growth [16,22].

The short-lived diffusive growth regime has thus far attracted little attention in the simulations of fluid-fluid spinodal decomposition, since the focus has been on the two later stages. In the lattice-based methods, which are specifically designed for the long length and time scales, the omission of the initial stage is self-evident. But for the off-lattice particle-based simulations, which by construction are limited to short length and time scales, the absence of studies on the initial $t^{1/3}$ regime is rather surprising. In this study, we concentrate on this first stage of spinodal decomposition and the subsequent transition to the viscous regime. We combine the best features of both above discussed particle based simulation techniques, to wit, the realistic hard interactions from MD and the momentum conserving thermostat from DPD. This paper is organized as follows: in Sec. II we briefly describe the employed simulation model and a technique to determine the average size of the emerging domains. Our simulation results are presented in Sec. III, followed in Sec. IV by a discussion and comparison with previous studies.

II. SIMULATION DETAILS

In our molecular dynamics simulations [25,26], the interaction between two like particles at a distance r is modeled by the Lennard-Jones (LJ) potential,

$$U_{\mathrm{LJ}}(r) = 4\epsilon \left[\left(\frac{\sigma}{r} \right)^{12} - \left(\frac{\sigma}{r} \right)^6 \right], \qquad (2)$$

where ϵ and σ are the strength and radius of the potential, respectively. The potential is smoothly truncated at the cutoff distance $r_c = 2.5\sigma$, to eliminate discontinuities in the energy and in the forces. Unlike particles interact by the same LJ potential in the preparatory equilibration runs and by the purely repulsive Weeks-Chandler-Andersen (WCA) potential, defined as $U_{\mathrm{WCA}}(r) = U_{\mathrm{LJ}}(r) + \epsilon$ for $r \leq 2^{1/6}\sigma$ and $U_{\mathrm{WCA}}(r) = 0$ for $r > 2^{1/6}\sigma$, during the phase separation simulations. The Verlet leap-frog algorithm is used to numerically integrate Newton's equations of motion with a time step $\Delta t = 0.002\tau$, where $\tau = \sqrt{m\sigma^2/\epsilon}$ is the natural LJ unit of time and m is the mass of a particle.

A thermostat is employed to maintain a constant temperature T throughout the simulation, mainly by dissipating the excess energy released by the phase separating system. The traditional MD thermostats based on velocity scaling [25,26] interfere with the evolution of the hydrodynamical flow field, and are therefore less suited for studying processes in which these flow fields might play an important role. We have therefore used a thermostat, introduced by Hoogerbrugge and Koelman [24] as part of the DPD method, which was particularly designed to obey Newton's third law and hence automatically gives rise to permissible flow fields. In summary, any two particles at a distance r within the cutoff radius r_c interact by friction and random forces [24,27,28],

$$\mathbf{F}_{\mathrm{thermo}} = -\frac{\kappa^2}{2k_B T} \left(1 - \frac{r}{r_c} \right)^2 (\hat{\mathbf{r}} \cdot \Delta \mathbf{v}) \hat{\mathbf{r}} + \frac{\kappa}{\sqrt{\Delta t}} \left(1 - \frac{r}{r_c} \right) \zeta \hat{\mathbf{r}}, \qquad (3)$$

where κ sets the activity of the thermostat, k_B is Boltzmann's constant, $\hat{\mathbf{r}}$ is the unit vector between the two particles, and $\Delta \mathbf{v}$ is their velocity difference. The random numbers ζ have zero average, unit standard deviation, are independent for every particle pair and are sampled every time step from a distribution without memory. A fluctuation-dissipation theorem relating the variances of the friction and random forces to the desired equilibrium temperature T has been included in the above equation. Note that the thermostatting forces do not affect the thermodynamic properties of the Lennard-Jones fluid, but they will slow down the dynamics of the fluid. We take advantage of this corollary by selecting a fairly high friction parameter, $\kappa = 3\epsilon\tau^{1/2}\sigma^{-1}$, to increase the length t_{dv} of the diffusive growth regime. This particular choice decreases the diffusion coefficient of the LJ particles by a factor of about 3 relative to the nonthermostatted fluid. A further convenient property of the DPD thermostat is that it couples to the local temperature, as opposed to conventional MD thermostats which act on the overall mean temperature. Note that we have not used the extremely soft potentials cointroduced with the DPD thermostat [24]: these

weak interactions lead to fluids with very low Schmidt numbers [27] and consequently reduce the span t_{dv} of the diffusive growth regime.

All simulations were performed using three-dimensional symmetric binary mixtures, containing a total of N $=500\,000$ particles in a cubic box with periodic boundary conditions. The number density was fixed at $\rho=0.7\sigma^{-3}$, yielding box sizes $L=89\sigma$. Every simulation started with the creation of a new homogeneous system, by randomly inserting particles in the simulation box and rejecting all insertions resulting in a large overlap with previously accepted particles. Next, these boxes were thoroughly equilibrated in MD simulations at the desired temperatures of $T=1\epsilon/k_B$, $2\epsilon/k_B$, and $3\epsilon/k_B$, using the same Lennard-Jones potential for all interactions to create homogeneous systems. Finally, phase separation was initiated by replacing the LJ interaction between unlike particles by the WCA potential, which instantaneously quenches the simulation boxes to states deeply below the spinodal. All particle coordinates $\mathbf{r}_j(t)$ were stored at intervals of 0.2τ for later visualization and analysis of the phase separation dynamics.

Since the time-dependent average domain size $R(t)$ is the most interesting and natural measure for the progression of the phase separation, we have determined this coarsening function from the structure factors of the stored configurations. The latter are calculated as

$$S(\mathbf{k},t) = \langle \hat{\phi}(\mathbf{k})\hat{\phi}(-\mathbf{k})\rangle, \qquad (4)$$

where the Fourier transform of the order field reads as

$$\hat{\phi}(\mathbf{k}) = \sum_{j=1}^{N} b_j e^{i\mathbf{k}\cdot\mathbf{r}_j(t)}, \qquad (5)$$

with $b_j = \pm 1$ depending on the type of particle j and $\mathbf{k}$ a wave vector commensurate with the box dimensions. Along any direction in reciprocal space, the structure factors of a symmetric binary liquid start at $S=0$ for $k=0$, then rise to a maximum S_m for wave number k_m before gradually returning to zero at large wave numbers. Since the structure factors $S(\mathbf{k},t)$ calculated from a single configuration at time t are rather noisy, we exploited this rotational symmetry to calculate spherically averaged structure factors $S_{\mathrm{sph}}(k,t)$, using a bin width of $\Delta k=0.017\sigma^{-1}$. The structure factors of four independent runs were averaged before making a least-squares fit with the scaling function

$$S_F(k,t) = S_m(t)\frac{3[k/k_m(t)]^2}{2+[k/k_m(t)]^6}, \qquad (6)$$

proposed by Furukawa [29] on the basis of the limiting behaviors of $S(k)$ at small and large k. One readily shows that this function reaches a maximum of $S_m(t)$ for the wave number $k=k_m(t)$. Note that Furukawa's function is consistent with the dynamical scaling hypothesis, which is expected to hold for the evolving phase separated domains. An offset in the wave number, introduced as a third fit parameter to improve the quality of fit [30], spoils this scaling invariance and is therefore not recommendable. The characteristic lengths of the domains in our simulations are finally extracted from the
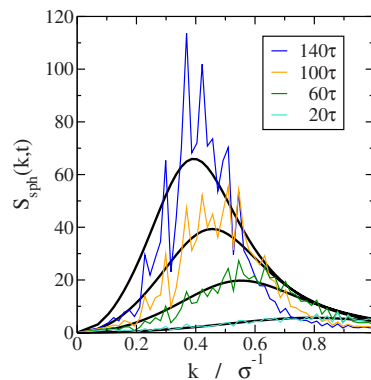

FIG. 1. (Color online) Spherically averaged structure factors $S_{\mathrm{sph}}(k,t)$ for four times, $t=20\tau$, 60τ, 100τ, and 140τ, after quenching a homogeneous system. The data shown are averages over four independent simulations to improve the signal-to-noise ratio. Thick smooth lines represent fits with the Furukawa function, see Eq. (6). As time advances, the position k_m of the peak shifts to lower wave numbers, and the height of the peak increases, indicating that the domains are growing.

peak positions of the fitted functions by $R(t)=2\pi/k_m(t)$. We believe that this route to the average domain size provides a worthwhile alternative to the more common approaches based on the first or second moment of $S(k)$, especially when the structure factors are compounded with noise.

III. RESULTS

Visual inspection of the stored trajectory files, using the visual molecular dynamics (VMD) package [31], vividly illustrates the sequence of events in a phase separating fluid mixture. Immediately following the quench, tiny domains of like particles appear throughout the previously homogeneously mixed system. The domains gradually increase in size until their diameters reach a significant fraction of the box dimensions, at which point the simulations are terminated. A quantitative measure of the domain sizes is obtained by calculating the spherically averaged structure factors $S_{\mathrm{sph}}(k,t)$ of the stored configurations, using the procedure outlined in the preceding section. Typical results for four distinct times during the phase separation are plotted in Fig. 1. In agreement with the visual inspection of the simulation movies, the position k_m of the peak gradually shifts toward lower wave numbers with increasing time. The four data sets are fitted reasonably well, see the thick lines in the plot, by the master curve proposed by Furukawa, see Eq. (6). A closer inspection reveals that the master curve systematically overestimates the structure factors in the tails at both sides of the peak. We want to emphasize that the quality of the fit function is of minor importance in the current analysis, provided both the emerging pattern and the applied fit function are in agreement with the dynamical scaling hypothesis. An average domain size R is now readily deduced from the peak position k_m, which is one of the two fit parameters in the Furukawa function. Since it proves difficult to make reliable fits of the structure factors at early times into the decompo-
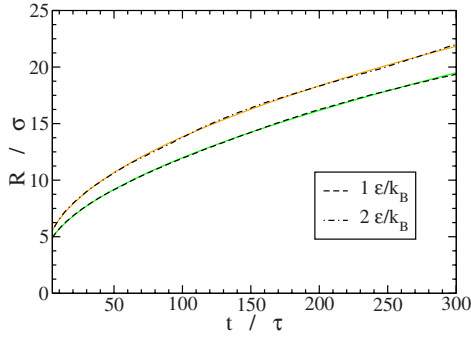
FIG. 2. (Color online) Characteristic length scale R of the phase separated domains, as deduced from the structure factors, plotted (in black) as a function of time for the two lower temperatures. The colored (gray) lines are fits with the generalized power law, see Eq. (7), whose fit parameters are listed in Table I.
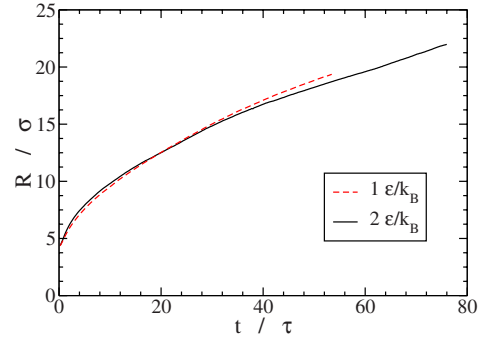

FIG. 3. (Color online) Characteristic length scale R of the phase separated domains plotted against scaled time, for the two lower temperatures. The growth curves are expected to coalesce in the viscous regime, after rescaling time with the temperature-dependent factor γ/η.

sition simulation, $t < 5\tau$, where the demixing has not yet yielded well-defined domains and the signal-to-noise ratio in the $S(k,t)$ is still unfavorable, we have omitted these earliest times in the following analysis.

The average domain sizes are plotted as functions of time in Fig. 2 for the two lowest temperatures, $T=1\epsilon/k_B$ and $T=2\epsilon/k_B$. Both curves show a sublinear regime at small times followed by a near-linear regime at later times, which we identify with the diffusive and viscous scaling regimes, respectively. Since the power laws of Eq. (1) were deduced from mesoscopic equations of motion, they are expected to hold true for mesoscopic time and length scales only. The current simulations, however, are at a level where the underlying microscopic details might be expected to be still relevant to the domain coarsening. It therefore appears appropriate to fit the observed growth functions with a more general power law [20],

$$R(t) = R_0 + a(t/\tau)^{\alpha}, \qquad (7)$$

where R_0 represents a microscopic offset in the domain size. The Lennard-Jones unit of time τ is introduced here for convenience, thus making the dimensions of a independent of the value of α. The resulting fit parameters are collected in Table I. Of particular interest are the two similar growth exponents of $\alpha \approx 0.55$, which suggests that we are sampling a time interval close to or surrounding the transition time t_{dv} from the diffusive $\alpha = 1/3$ to the viscous $\alpha = 1$ growth regime. It is tempting, therefore, to extract from the simulated

TABLE I. Parameters obtained by fitting the simulated growth functions at three temperatures with the power law of Eq. (7). In the last line, the growth for $t \geq 100\tau$ was fitted with a simple power law, i.e., without the offset R_0.

$T/\epsilon k_B^{-1}$	R_0/σ	a/σ	α
1	3.37	0.62	0.57
2	3.33	0.97	0.52
3	−1.85	4.96	0.27
3		4.10	0.28

range an initial and a late period; the bounds on these periods are admittedly rather arbitrary in the absence of a clear transition. By fitting the growth curve at $T=2\epsilon/k_B$ over the initial period $5\tau \leq t \leq t_i$, with $t_i = 50\tau$, 25τ, and 15τ, we find the substantially lower exponents of $\alpha = 0.45$, 0.39, and 0.40, respectively. These values hint at a transient regime with diffusion-limited growth, although the covered time interval is far too short to admit a more definitive conclusion. The other two fit parameters are also fairly consistent in these three regions, with $R_0 \approx 2.0\sigma$ and $a \approx 1.9\sigma$. At the lower temperature of $T=1\epsilon/k_B$, the exponent remains almost unaltered at $\alpha \approx 0.55$ for all tested upper bounds on the initial range, implying that the diffusive region is extremely short lived in this case. In the final region of the growth curve, $t_f \leq t \leq 300\tau$ with t_f between 150τ and 250τ, it proves difficult to fit the data with a general power law. The growth exponents are found to vary strongly with t_f, yielding values as disparate as 0.24 and 1.57, while the other two fit parameters are equally inconsistent, making the direct evaluation of the growth exponent unreliable in this regime. Laradij et al. [20] identify the viscous growth process in their simulations by noting that rescaling of the curves at different temperatures according to the predicted growth law, $R \propto \gamma t/\eta$, should make the curves coalesce. We calculate the interfacial tension from the difference in the pressures parallel and perpendicular to the fluid-fluid interface in a phase separated box with two flat interfaces [26,27]. The viscosity is extracted from the self-diffusion coefficient D in the homogeneous liquid by using the Stokes-Einstein expression, $D=k_BT/c\pi\eta R$, with $c=5$ and $R=\sigma/2$ [32]. Both calculations are performed at $T=1\epsilon/k_B$ and $2\epsilon/k_B$. After rescaling both growth curves by their respective factors, we observe the good agreement depicted in Fig. 3. Plots of $R(t)$ against $t^{1/3}$, the predicted power law in the diffusive regime, yield a less satisfactory agreement between the two curves, even if the value of the undetermined diffusive transport coefficient λ is chosen such as to minimize the differences between the curves (not shown). Rescaling both growth curves according to the inertial law produces a clear deviation between the graphs (not shown). Taken together, this strongly indicates that the observed growth of the average domain size is best characterized as being in the viscous regime.
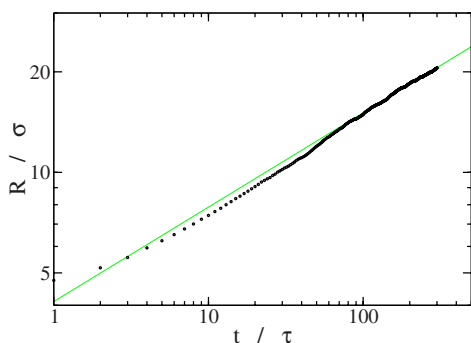
FIG. 4. (Color online) Average domain size during spinodal decomposition at the elevated temperature of $T=3\epsilon/k_B$. The slope α $=0.29$ of the fitted line is in good agreement with the $\alpha=1/3$ expected in a diffusive growth process.

A completely different picture emerges at the higher temperature of $T=3\epsilon/k_B$. Fitting the data with the general power law, see Table I, we find that the average domain size grows with an exponent $\alpha=0.27$ over the entire simulated time interval. On a double logarithmic plot, presented in Fig. 4, the curve converges to the straight line $R=4.1\sigma(t/\tau)^{0.28}$, fitted over the range $100\tau \lesssim t \lesssim 300\tau$. These exponents are in good agreement with the $\alpha=1/3$ predicted for the diffusive regime.

IV. DISCUSSION AND CONCLUSIONS

The initial stages of phase separation in a quenched homogeneous mixture of immiscible binary fluids have been studied by molecular dynamics simulations. At the elevated temperature of $T=3\epsilon/k_B$, the power-law growth of the average domain size is in good agreement with the initial diffusive growth mechanism $R \propto t^{1/3}$ predicted by the Lifshitz-Slyozov theory. This is the first clear observation of the diffusive regime in three-dimensional molecular dynamics simulations of spinodal decomposition. For the intermediate temperature of $T=2\epsilon/k_B$ the diffusive regime is short lived, and quickly gives way to a viscous regime. The latter is the only regime discernible in the simulations at the low temperature of $T=1\epsilon/k_B$. Although an accurate growth exponent cannot be established, the characterization of this regime is supported by the observed scaling behavior with temperature.

The small mean domain sizes in the initial parts of the simulations, for $R(t) \lesssim L/10 \sim 10\sigma$, imply that the simulation boxes contain a large number of domains, be they correlated. In combination with the averaging over four unrelated simulations at every temperature, this suggests that the temporal evolution of the mean domain size has been determined accurately for short times. Since the average repeat distance of the phase separated domains remains relatively small compared to the box dimensions until the termination of the runs, $R(t) \lesssim L/4$ for all t, possible box-size related artifacts are

expected to be still of minor importance. The accuracy of $R(t)$ will, however, decrease at the later times, which might contribute to the difficulties in determining the growth exponent in the viscous regime.

The introduction of a domain size offset R_0 in the general power law, as proposed by Laradji *et al.* [20], is important for the quality of the fit, especially since the actually attained mean domain sizes are not orders of magnitude larger than R_0. We find that this offset for the two lowest temperatures is of the same magnitude as the sizes of the particles, which agrees with the intuition of a viscous growth process starting from small clusters. An additional temporal offset t_0 was introduced in some fits, replacing t by $t-t_0$ on the right-hand side of Eq. (7). We found that this did not substantially improve the quality of the fit, with t_0 often being close to zero. A number of fits even became numerically poorly defined, indicative of the redundancy introduced by the extra degree of freedom.

The transition time t_{dv} between diffusive and viscous growth is seen to increase strongly with increasing temperature. At $T=1\epsilon/k_B$ there is no clear transition, for $T=2\epsilon/k_B$ we estimate $t_{dv} \sim 50\tau$, while at $T=3\epsilon/k_B$ the transition is not even reached within the spanned time range, i.e., $t_{dv} > 300\tau$. We suggest that critical slowing down plays an important role in the pronounced rise of t_{dv} with T. Simulations at the higher temperature $T=3.5\epsilon/k_B$ show a limited transient degree of clustering but do not yield a continuous growth of these clusters, implying that this temperature already exceeds the critical temperature. It cannot be ruled out, however, that the effect reflects a steep temperature dependence of λ. Further calculations, exceeding the scope of this paper, are required to investigate these possible explanations. A simple calculation yields that $t_{vi}^* \approx 100\tau$ at $T=2\epsilon/k_B$, which in combination with the previously established $t_{vi} \sim 10^4 t_{vi}^*$ explains why the inertial regime is not observed in the current simulations.

The transition time t_{dv} is also interesting for the study of spinodal decompositions of liquid mixtures exposed to a shear deformation [33,34]. At relatively low shear rates, $\dot{\gamma} < t_{dv}^{-1}$, the effect of the flow is sufficiently small for well-defined domains to form. The flow deformation will distort the domains, possibly tearing them apart, but may also be effective in bringing domains together. For relatively high shear rates, $\dot{\gamma} > t_{dv}^{-1}$, the deformation flow is expected to compete with the diffusive stage of phase separation, thus seriously hindering the formation of clear domains. In a forthcoming paper we will discuss this competition between phase separation and flow deformation, for the current Lennard-Jones liquid, in a Couette geometry.

[1] J. D. Gunton, M. San Miguel, and P. S. Sahni, in *Phase Transitions and Critical Phenomena*, edited by C. Domb and J. L. Lebowitz (Academic, New York, 1983), Vol. 8, p. 267.

[2] H. Tanaka, J. Phys.: Condens. Matter **12**, R207 (2000).

[3] A. J. Bray, Adv. Phys. **43**, 357 (1994).

[4] P. C. Hohenberg and B. I. Halperin, Rev. Mod. Phys. **49**, 435 (1977).

[5] I. M. Lifshitz and V. V. Slyozov, J. Phys. Chem. Solids **19**, 35 (1961).

[6] E. D. Siggia, Phys. Rev. A **20**, 595 (1979).

[7] H. Furukawa, Phys. Rev. A **31**, 1103 (1985).

[8] V. M. Kendon, Phys. Rev. E **61**, R6071 (2000).

[9] Y. C. Chou and W. I. Goldburg, Phys. Rev. A **20**, 2105 (1979).

[10] N. C. Wong and C. M. Knobler, J. Chem. Phys. **69**, 725 (1978).

[11] N. C. Wong and C. M. Knobler, Phys. Rev. A **24**, 3205 (1981).

[12] N. A. M. Verhaegh, J. S. van Duijneveldt, J. K. G. Dhont, and H. N. W. Lekkerkerker, Physica A **230**, 409 (1996).

[13] S. Puri and B. Dünweg, Phys. Rev. A **45**, R6977 (1992).

[14] V. M. Kendon, J. C. Desplat, P. Bladon, and M. E. Cates, Phys. Rev. Lett. **83**, 576 (1999).

[15] F. J. Alexander, S. Chen, and D. W. Grunau, Phys. Rev. B **48**, 634 (1993).

[16] C. Appert, J. F. Olson, D. H. Rothman, and S. Zaleski, J. Stat. Phys. **81**, 181 (1995).

[17] V. M. Kendon, M. E. Cates, I. Pagonabarraga, J. C. Desplat, and P. Bladon, J. Fluid Mech. **440**, 147 (2001).

[18] P. J. Love, P. V. Coveney, and B. M. Boghosian, Phys. Rev. E **64**, 021503 (2001).

[19] W. J. Ma, A. Maritan, J. R. Banavar, and J. Koplik, Phys. Rev. A **45**, R5347 (1992).

[20] M. Laradji, S. Toxvaerd, and O. G. Mouritsen, Phys. Rev. Lett. **77**, 2253 (1996).

[21] H. Kabrede and R. Hentschke, Physica A **361**, 485 (2006).

[22] P. V. Coveney and K. E. Novik, Phys. Rev. E **54**, 5134 (1996).

[23] S. I. Jury, P. Bladon, S. Krishna, and M. E. Cates, Phys. Rev. E **59**, R2535 (1999).

[24] P. J. Hoogerbrugge and J. M. V. A. Koelman, Europhys. Lett. **19**, 155 (1992).

[25] M. P. Allen and D. J. Tildesley, *Computer Simulation of Liquids* (Oxford University Press, Oxford, UK, 1987).

[26] D. Frenkel and B. Smit, *Understanding Molecular Simulations. From Algorithms to Applications*, 2nd ed. (Academic, San Diego, CA, 2002).

[27] R. D. Groot and P. B. Warren, J. Chem. Phys. **107**, 4423 (1997).

[28] W. K. den Otter and J. H. R. Clarke, in *Simulation Methods for Polymers*, edited by M. J. Kotelyanskii and D. N. Theodorou (Marcel Dekker, New York, 2004), pp. 559–574.

[29] H. Furukawa, Physica A **123**, 497 (1984).

[30] S. Y. Trofimov, Ph.D. thesis, Eindhoven University of Technology, 2003.

[31] W. Humphrey, A. Dalke, and K. Schulten, J. Mol. Graph. **14**, 33 (1996).

[32] M. Cappelezzo, C. A. Caperllari, S. H. Pezzin, and L. A. F. Coelho, J. Chem. Phys. **126**, 224516 (2007).

[33] A. Onuki, J. Phys.: Condens. Matter **9**, 6119 (1997).

[34] P. Padilla and S. Toxvaerd, J. Chem. Phys. **106**, 2342 (1997).